Journal of Computational Mathematics
Vol.31, No.2, 2013, 154–174.

http://www.global-sci.org/jcm
doi:10.4208/jcm.1210-m3799

A SECOND ORDER MODIFIED CHARACTERISTICS VARIATIONAL MULTISCALE FINITE ELEMENT METHOD FOR TIME-DEPENDENT NAVIER-STOKES PROBLEMS*

Zhiyong Si
School of Mathematics and Information Science, Henan Polytechnic University, Jiaozuo 454003, China
Email: sizhiyong@yahoo.com.cn
Jian Su Yinnian He
Center for Computational Geosciences, School of Mathematics and Statistics, Xi'an Jiaotong University, Xi'an 710049, China
Email:jsu@mail.xjtu.edu.cn heyn@mail.xjtu.edu.cn

Abstract

In this paper, by combining the second order characteristics time discretization with the variational multiscale finite element method in space we get a second order modified characteristics variational multiscale finite element method for the time dependent Navier-Stokes problem. The theoretical analysis shows that the proposed method has a good convergence property. To show the efficiency of the proposed finite element method, we first present some numerical results for analytical solution problems. We then give some numerical results for the lid-driven cavity flow with Re = 5000, 7500 and 10000. We present the numerical results as the time are sufficient long, so that the steady state numerical solutions can be obtained.

Mathematics subject classification: 76D05, 76M10, 65M60, 65M12.
Key words: Modified method of characteristics, Defect-correction finite element method, Navier-Stokes problems, Characteristics-based method, Lid-driven problem.

1. Introduction

Finding efficient numerical methods for the Navier-Stokes equation is a key component in the incompressible flow simulation. There are a few efficient iterative methods for solving the stationary Navier-Stokes equations under some strong uniqueness conditions presented by some authors, see, e.g., [21,23,24]. It is known that variational multiscale (VMS) method is an efficient method for solving the high Reynolds Navier-Stokes equations. The basic idea of the VMS method is to splitting the solution into resolved and unresolved scale, representing the unresolved scales in terms of the resolved scales, and using this representation in the variational equation for the resolved scales. In [26, 27], Hughes and his coworkers presented the VMS method firstly. After then, there are many works devoted to this method, e.g., VMS method for the Navier-Stokes equations [31]; a two-level VMS methods for convection-dominated diffusion problems [32]; VMS methods for turbulent flows [13, 34, 35]; large-eddy simulation (LES) [28, 29, 37]; subgrid-scale models for the incompressible flow [26, 46]. There is another class of VMS methods which rely on a three-scale decomposition of the flow field into large, resolved small and unresolved scales [12]. By the difference of the definition of the large-scale projections,

* Received July 29, 2011 / Revised version received September 10, 2012 / Accepted October 25, 2012 / Published online March 14, 2013 /

the VMS methods can be classified into two kinds. In [33, 36], John et al. presented the error analysis of these two kinds of VMS methods for the Navier-Stokes equations.

The characteristics method, in which the hyperbolic part (the temporal and advection term) is treated by a characteristic tracking scheme, is a highly effective method for advection dominated problems. There are many authors devoted to this method, see, e.g., [1, 2, 4, 6, 9, 10, 15, 22, 42, 45]. In [16], Douglas and Russell presented the modified method of characteristics (MMOC) firstly. A characteristics mixed finite element method for advection-dominated transport problems was presented by Arbogast [2]. Russell [41] extended it to nonlinear coupled systems in two and three spacial dimensions. In [39], a detail analysis for the Navier-Stokes equations is provided by Pironneau. He obtained suboptimal convergence rates of the form $\mathcal{O}(h^m + \triangle t + h^{m+1}/\triangle t)$, which is improved by Dawson et al [14]. In [5], Boukir et al. presented a second-order time scheme based on the characteristics method and spatial discretization of finite element type for the incompressible Navier-Stokes equations. An optimal error estimate for the Lagrange-Galerkin mixed finite element approximation of the Navier-Stokes equations was given by Süli in [44]. The second order in time method for linear convection diffusion problems had been given by Ewing and Russell [18]. In [43], a second order MMOC mixed defect-correction finite element method for time dependent Navier-Stokes problems was proposed.

In this paper, we present a second order modified characteristics VMS finite element method for time dependent Navier-Stokes equations. In our method, the hyperbolic part (the temporal and advection term) is treated by a second order characteristic tracking scheme. Then we use VMS based on projection finite element method in space discretization. The error analysis shows that this method has a good convergence property. In order to show the efficiency of the second order MCVMS finite element method, we first present some numerical results of an analytical solution problems. The numerical results show that the convergence rates are $\mathcal{O}(h^3)$ of the L^2-norm for u, $\mathcal{O}(h^2)$ of the semi H^1-norm for u and $\mathcal{O}(h^2)$ of the L^2-norm for p, which agrees very well with our theoretical results by using $P_2 - P_1$ finite element spaces. Then, some numerical results of the lid-driven cavity flow with $Re = 5000$ and 7500 were given, firstly. We present the numerical results as the time are sufficient long enough. By the numerical results, we can see that a steady state numerical solutions of the the time-dependent Navier-Stokes equations were obtained. Meanwhile, the numerical solutions are in good agreement with that of the steady Navier-Stokes equations shown by Ghia et al. [20] and Erturk et al. [17]. At last, we present some numerical results for $Re = 10000$. It shows that the solution is quasi-periodic and has small variations at the monitoring point. The phase portraits of the monitoring points show that the variations in amplitude yield a solution which is quasi-periodic. It is observed from these numerical results that the schemes can results in good accuracy and is highly efficient.

2. Functional Setting of the Navier-Stokes Equations

In this paper, we consider the time-dependent Navier-Stokes(NS) problems

$$\begin{cases} u_t - \nu \triangle u + (u \cdot \nabla) u + \nabla p = f, & x \in \Omega \times [0, T], \\ \nabla \cdot u = 0, & x \in \Omega \times [0, T], \\ u(x, 0) = u_0(x), & x \in \Omega, \\ u(x, t) = 0, & x \in \partial\Omega \times [0, T], \end{cases} \tag{2.1}$$

where Ω is a bounded domain in $\mathbb{R}^2$ assumed to have a Lipschitz continuous boundary $\partial\Omega$. $u = (u_1(x,t), u_2(x,t))$ represents the velocity vector, $p(x,t)$ the pressure, $f(x,t)$ the body force, $\nu = 1/Re$ the viscosity number, Re the Reynolds number, respectively.

In this section, we first describe some of the notations and results which will be frequently used in this paper. We will use the Sobolev spaces

$$H^n(0,T;\Phi) = \left\{ v \in \Phi; \int_0^T \sum_{0\le i\le n} \left(\left\| \frac{\partial^i v}{\partial t^i} \right\|_\Phi \right)^2 dt < +\infty \right\},$$

equipped with the norm

$$\|v\|_{H^n(0,T;\Phi)} = \sum_{0\le i\le n} \left[\int_0^T \left(\left\| \frac{\partial^i v}{\partial t^i} \right\|_\Phi \right)^2 dt \right]^{\frac{1}{2}},$$

where Φ is a Hilbert space with the norm $\|\cdot\|_\Phi$. Especially, when $n = 0$ we note

$$\|v\|_{L^2(0,T;\Phi)} = \left(\int_0^T \|v\|_\Phi^2 dt \right)^{\frac{1}{2}}.$$

We also define

$$L^\infty(0,T;\Phi) = \left\{ v \in \Phi;\ \text{ess} \sup_{0\le t\le T} \|v\|_\Phi < +\infty \right\},$$

with the norm

$$\|v\|_{L^\infty(0,T;\Phi)} = \text{ess} \sup_{0\le t\le T} \|v\|_\Phi.$$

The following Hilbert spaces will be used

$$\begin{aligned} X &:= H_0^1(\Omega)^2, \\ M &:= L_0^2(\Omega) = \left\{ \varphi \in L^2(\Omega); \int_\Omega \varphi dx = 0 \right\}, \\ V &:= \Big\{ v \in X; (\nabla \cdot v, q) = 0, \forall q \in M \Big\}. \end{aligned}$$

The following assumptions and results are recalled (see [24]).

($\mathbf{A_1}$) There exists a constant C_0 which only depends on Ω, such that

(*i*) $\|u\|_0 \le C_0 \|\nabla u\|_0,\ \|u\|_{0,4} \le C_0 \|\nabla u\|_0,\ \forall\ u \in H_0^1(\Omega)^2(\text{or } H_0^1(\Omega))$,

(*ii*) $\|u\|_{0,4} \le C_0 \|u\|_1,\ \forall\ u \in H^1(\Omega)^2$,

(*iii*) $\|u\|_{0,4} \le \sqrt{2} \|\nabla u\|_0^{\frac{1}{2}} \|u\|_0^{\frac{1}{2}},\ \forall\ u \in H_0^1(\Omega)^2(\text{or } H_0^1(\Omega))$.

Here, $\|\cdot\|_0$ and $\|\cdot\|_{0,4}$ are L^2 and L^4 norms respectively.

($\mathbf{A_2}$) Assume that Ω is smooth, hence the unique solution $(v,q) \in (X,M)$ of the steady Stokes problem

$$\begin{aligned} &-\triangle v + \nabla q = g, \nabla \cdot v = 0, \text{ in } \Omega, \\ &v|_{\partial\Omega} = 0, \end{aligned}$$

for any prescribed $g \in L^2(\Omega)^2$ exits and satisfies

$$\|v\|_2 + \|q\|_1 \le c\|g\|_0,$$

where $c > 0$ is a generic constant depending on Ω, which may stand for different values at its different occurrences.

3. Second Order MCVMS Finite Element Methods

3.1. Semi-discrete VMS FEMs for time-dependent NS equations

Let $\Im_h$ be a semi-uniform partition of $\bar{\Omega}$ into non-overlapping triangles, indexed by a parameter $h = \max_{K\in\Im_h}\{h_K; h_K = \text{diam}(K)\}$. We introduce the finite element subspace $X_h \subset X, M_h \subset M$ as follows

$$X_h = \Big\{v_h \in X \cap C^0(\bar{\Omega})^2; v_h|_K \in P_\ell(K)^2, \forall K \in \Im_h\Big\},$$
$$M_h = \Big\{q_h \in M \cap C^0(\bar{\Omega}); q_h|_K \in P_k(K), \forall K \in \Im_h\Big\},$$

where $P_\ell(K)$ is the space of piecewise polynomials of degree ℓ on K, $\ell \geqslant 1, k \geqslant 1$ are two integers. We assume that (X_h, M_h) satisfies the discrete LBB condition

$$\sup_{v_h\in X_h} \frac{d(\varphi_h, v_h)}{\|\nabla v_h\|_0} \geqslant \beta\|\varphi_h\|_0, \quad \forall \varphi_h \in M_h. \tag{3.1}$$

where $d(\varphi, v) = (\varphi, \nabla\cdot v)$. V_h is the kernel of the discrete divergence operator

$$V_h = \Big\{v_h \in X_h; (q_h, \nabla\cdot v_h) = 0, \forall q_h \in M_h\Big\}.$$

For the VMS finite element methods, a large scale space $L_H \subset L = \{\mathbb{L} \in (L^2(\Omega))^{2\times 2}, \mathbb{L} = \mathbb{L}^T\}$ and a so-called turbulent viscosity $\nu_T \geq 0$ are introduced. The semi-discrete problems reads as follows (please see [35]): Find $u_h : [0,T] \to V_h, p_h : [0,T] \to M_h$ and $\mathbb{G}_H : [0,T] \to L_H$ satisfying

$$\begin{aligned}
&(u_{ht}, v_h) + (\nu + \nu_T)a(u_h, v_h) - d(p_h, v_h) + b(u_h, u_h, v_h) + d(\varphi_h, u_h)\\
&\qquad -(\nu_T \mathbb{G}_H, \nabla v_h) = (f, v_h) \quad \forall v_h \in X_h, \varphi_h \in M_h,\\
&(\mathbb{G}_H - \nabla u_h, \mathbb{L}_h) = 0, \quad \forall \mathbb{L}_H \in L_H,
\end{aligned} \tag{3.2}$$

where $a(u,v) = (\nabla u, \nabla v)$,

$$b(u,v,w) = \frac{1}{2}\left[\int_\Omega \sum_{i,k=1}^{2} u_i \frac{\partial v_k}{\partial x_i} w_k dx - \int_\Omega \sum_{i,k=1}^{2} u_i \frac{\partial w_k}{\partial x_i} v_k dx\right],$$

and $u_h(x,0) = u_h^0 \in V_h$ is a discretely divergence free approximation of u_0. Let $P_{L_H} : L \to L_H$ denote the L^2-projection from L onto L_H, for all $l \in L$

$$(P_{L_H} l - l, \mathbb{L}_H) = 0, \quad \forall \mathbb{L}_H \in L_H. \tag{3.3}$$

Therefore, $\mathbb{G}_H = P_{L_H}\nabla u_h$ in (3.2). Since P_{L_H} is an L^2-projection, it follows for $v \in V$ and $\|\nabla v\|_0 > 0$,

$$\begin{aligned}
\nu_T\|(I - P_{L_H})\nabla v\|_0^2 &= \nu_T\left(\|\nabla v\|_0^2 - \|P_{L_H}\nabla v\|_0^2\right)\\
&= \nu_T\left(1 - \frac{\|P_{L_H}\nabla v\|_0^2}{\|\nabla v\|_0^2}\right)\|\nabla v\|_0^2 \equiv \nu_{add}\|\nabla v\|_0^2.
\end{aligned} \tag{3.4}$$

By $0 \leq \|P_{L_H}\nabla v\|_0 \leq \|\nabla v\|_0$, we get

$$0 \leq \nu_{add} \leq \nu_T. \tag{3.5}$$

By straightforward calculation, we can deduce

$$(\nu_T \nabla u_h, \nabla v_h) - (\nu_T P_{L_H} \nabla u_h, \nabla v_h) = (\nu_T (I - P_{L_H}) \nabla u_h, (I - P_{L_H}) \nabla v_h). \tag{3.6}$$

Hence, system (3.2) can be reformulated as: Find $u^h : [0,T] \to V_h, p^h : [0,T] \to M_h$ satisfying

$$\begin{aligned}&(u_{ht}, v_h) + \nu a(u_h, v_h) + b(u_h, u_h, v_h) - d(p_h, v_h) + d(\varphi_h, u_h)\\&\quad + (\nu_T (I - P_{L_H}) \nabla u_h, (I - P_{L_H}) \nabla v_h)\\&= (f, v_h), \quad \forall v_h \in X_h, \varphi_h \in M_h.\end{aligned} \tag{3.7}$$

3.2. Second order MC-mixed FEMs and the second order MCVMSFEM for the NS equations

For each positive integer N, let $\{\mathcal{J}_n : 1 \le n \le N\}$ be a partition of $[0,T]$ into subintervals $\mathcal{J}_n = (t_{n-1}, t_n]$, with $t_n = n\triangle t$, $\triangle t = T/N$. Set $u^n = u(\cdot, t_n)$. We focus our study on a second-order approximation suggested by Ewing et al. [18] and Boukir et al. [5], set

$$\tilde{x} = x - u^{n*}(x)\triangle t, \tag{3.8}$$

$$\tilde{\tilde{x}} = x - 2u^{n*}(x)\triangle t, \tag{3.9}$$

where $u^{n*} = 2u^n - u^{n-1}, u^{-1} = u_0$. Consequently, the hyperbolic part in the first equation of (2.1) at time t_n is approximated by

$$u_t(t_n) + u^{n-1} \cdot \nabla u^n \approx \frac{3u^{n+1} - 4\tilde{u}^n + \tilde{\tilde{u}}^{n-1}}{2\triangle t},$$

where

$$\tilde{w} = \begin{cases} w(\tilde{x}), & \tilde{x} = x - u^{n*}(x)\triangle t \in \Omega, \\ 0, & \text{otherwise}, \end{cases}$$

$$\tilde{\tilde{u}} = \begin{cases} u(\tilde{\tilde{x}}), & \tilde{\tilde{x}} = x - 2u^{n*}(x)\triangle t \in \Omega, \\ 0, & \text{otherwise}, \end{cases}$$

for any function w, u.

With the previous notations, we get the second order MMOCMFEM for the time-dependent Navier-Stokes (2.1): find $(u_h^n, p_h^n) : \{t_1, \ldots, t_N\} \to V_h \times M_h$ such that

$$\begin{aligned}&\left(\frac{3u_h^{n+1} - 4\bar{u}_h^n + \bar{\bar{u}}_h^{n-1}}{2\triangle t}, v_h\right) + \nu a(u_h^n, v_h) - d(p_h^n, v_h) + d(\varphi_h, u_h^n) = (f^n, v_h),\\&\qquad\qquad \forall v_h \in X_h, \varphi_h \in M_h,\end{aligned} \tag{3.10}$$

where $\bar{w} = w(\bar{x}), \bar{\bar{u}} = u(\bar{\bar{x}})$ and $\bar{x} = x - u_h^{n*}(x)\triangle t, \bar{\bar{x}} = x - 2u_h^{n*}(x)\triangle t, u_h^{n*} = 2u_h^n - u_h^{n-1}, u_h^{-1} = u_h^0$.

The MMOC time discretization, combined with the VMS finite element method in space, leads to the following second order MCVMS finite element method: Find $(u_h^n, p_h^n) \in (X_h \cap V_h) \times M_h$ at $t = t_n, n \geqslant 1$ such that

$$\begin{aligned}&\left(\frac{3u_h^{n+1} - 4\bar{u}_h^n + \bar{\bar{u}}_h^{n-1}}{2\triangle t}, v_h\right) + (\nu + \nu_T) a(u_h^{n+1}, v_h) - d(p_h^{n+1}, v_h)\\&\quad + d(\varphi_h, u_h^{n+1}) - (\nu_T \mathbb{G}_H^{n+1}, \nabla v_h) = (f^{n+1}, v_h), \quad \forall v_h \in X_h, \varphi_h \in M_h,\\&(\mathbb{G}_H^n - \nabla u_h^n, \mathbb{L}_H) = 0, \quad \forall \mathbb{L}_H \in L_H.\end{aligned} \tag{3.11}$$

Using (3.6), (3.11) can be reformulated as

$$\begin{aligned}&\left(\frac{3u_h^{n+1}-4\bar{u}_h^n+\bar{\bar{u}}_h^{n-1}}{2\triangle t},v_h\right)+\nu a(u_h^{n+1},v_h)-d(p_h^{n+1},v_h)+d(\varphi_h,u_h^{n+1})\\&\quad+(\nu_T(I-P_{L_H})\nabla u_h^{n+1},(I-P_{L_H})\nabla v_h)=(f^{n+1},v_h),\quad\forall v_h\in X_h,\varphi_h\in M_h.\end{aligned}\tag{3.12}$$

Remark 3.1 (i). Since L_H has been distinguish between resolved small scales and large scales, with L_H representing the large scales, it must be in some sense a coarse finite element space. One way of achieving this is by choosing it to be a lower order finite element space than V_h on the same grid. The other way is defining L_H on a coarser grid. This two methods are called one-level and two level projection-based FEVMS methods respectively (see [32, 35]).

(ii). The so-called turbulent viscosity ν_T can be chosen in many ways. In this paper we choose it in two ways (Smagorinsky-type [31])

$$\nu_T=\delta h^2\|\nabla u_h\|_0,\tag{3.13}$$

$$\nu_T=\delta h^2\|\nabla u_h-\mathbb{G}_H\|_0.\tag{3.14}$$

Remark 3.2 ([40,46]) If $L_H=\left\{l_H\in(C^0(\Omega))^{2\times2}:\ l_H|_K\in(P_k(K))^{2\times2},\ \forall K\in\Im_h\right\}$, then we have the following properties

$$\|P_{L_H}l\|_1\le C\|l\|_1,\qquad\forall l\in L,\tag{3.15}$$

$$\|(I-P_{L_H})l\|_0\le C\|\nabla l\|_0,\quad\forall l\in L,\tag{3.16}$$

$$\|l-P_{L_H}l\|_1\le Ch^l\|l\|_{l+1},\quad 1\le l\le k,\ \forall l\in H^{l+1}(\Omega)^{2\times2}\cap L.\tag{3.17}$$

4. Error Estimate

In order to provide the error analysis, we need the following lemmas.

Lemma 4.1. ([5]) *Let*

$$e(x,n)=\left[\frac{3u^{n+1}-4\tilde{u}^n+\tilde{\tilde{u}}^{n-1}}{2\triangle t}-\left(\frac{\partial u}{\partial t}(x,t_{n+1})+u^{n+1}(x)\nabla u^{n+1}(x)\right)\right]$$

and $\tau>0$ such that $u\in[\mathscr{C}^4([\tau,T];H^3(\Omega)^2]$. For $t_n>\tau$, we have

$$e(x,n)=-\triangle t^2\left(\frac{1}{3}\frac{d^3g_x^{n+1}}{dt^3}+\frac{\partial^2u}{\partial t^2}\cdot\nabla u(x,t_{n+1})\right)+O(\triangle t^3),\tag{4.1}$$

where $g_x^{n+1}(t)=u(x-(t_{n+1}-t)u^{n*},t),u^{n+1}(x)=u(x,t_{n+1})$.

Lemma 4.2. ([5]) *Let*

$$\tilde{e}(x,n)=\left(\frac{3u^{n+1}-4\tilde{u}^n+\tilde{\tilde{u}}^{n-1}}{2\triangle t}-\nu\triangle u^{n+1}(x)+\nabla p^{n+1}(x)-f^{n+1}(x)\right).\tag{4.2}$$

Let $\tau>0$ such that $u\in[\mathscr{C}^4([\tau,T];H^3(\Omega)^2]$. For $t_n>\tau$, we have

$$\tilde{e}(x,n)=-\triangle t^2\left(\frac{1}{3}\frac{d^3g_x^{n+1}}{dt^3}+\frac{\partial u}{\partial t}\cdot\nabla u(x,t_{n+1})\right)+O(\triangle t^3),\tag{4.3}$$

where $g_x^{n+1}(t)=u(x-(t_{n+1}-t)u^{n*},t),\ u^{n+1}(x)=u(x,t_{n+1})$.

We then define the Galerkin projection $(R_h, Q_h) = (R_h(u,p), Q_h(u,p)) : (X, M) \to (X_h, M_h)$, such that

$$\nu a(R_h - u, v_h) - d(Q_h - p, v_h) + d(\varphi_h, R_h - u) = 0,$$
$$\forall (u,p) \in (X, M), \ \ (v_h, \varphi_h) \in (X_h, M_h). \tag{4.4}$$

Lemma 4.3. ([25,38]) *The Galerkin projection (R_h, Q_h) satisfies, for $k = 1, 2$,*

$$\nu \|R_h - u\|_0 + h(\nu \|\nabla (R_h - u)\|_0 + \|Q_h - p\|_0) \le C h^{k+1} \Big(\nu \|u\|_{k+1} + \|p\|_k \Big). \tag{4.5}$$

Lemma 4.4. *The Galerkin projection (R_h, Q_h) satisfies*

$$\|R_h\|_\infty \le C\|u\|_\infty + Ch^k \|u\|_{H^{k+1}(\Omega)}. \tag{4.6}$$

Proof. We introduce the interpolation operator I_h and the element $I_h u$. By the triangle inequality, we deduce

$$\|R_h\|_\infty \le \|I_h u\|_\infty + \|R_h - I_h u\|_\infty.$$

Using the inverse inequality $\|v_h\|_\infty \le Ch^{-1}\|v_h\|_0$ yields (see [11])

$$\begin{aligned} \|R_h\|_\infty &\le \|I_h u\|_\infty + Ch^{-1}\|R_h - I_h u\|_0 \\ &\le \|I_h u\|_\infty + Ch^{-1}\Big(\|R_h - u\|_0 + \|u - I_h u\|_0 \Big). \end{aligned}$$

By (4.5) and the L^∞ stability of the interpolation operator [11] we complete the proof. $\square$

Lemma 4.5. *Let u_h^n be defined by* (3.12)*. If*

$$\triangle t \le \frac{1}{2L_n}, \quad L_n = \max_{1\le l \le n} \|u_h^{l*}\|_\infty, \quad \forall 1 \le n \le N-1, \tag{4.7}$$

then we have

$$\|u_h^{n+1}\|_\infty \le C, \tag{4.8a}$$

$$\begin{aligned} \|\xi_h^{n+1}\|_0^2 + \nu \triangle t \sum_{i=1}^{n+1} \|\nabla \xi_h^i\|_0^2 &\le C \exp(CT)\Big(\triangle t^4 + h^{2k+2} + \nu_{add} h^{2k} \Big) \\ &+ C \exp(CT) \left(\nu_T \triangle t \sum_{i=1}^{n+1} \|(I - P_{L_H})\nabla u^{i+1}\|_0^2 \right), \end{aligned} \tag{4.8b}$$

where $\xi_h^{n+1} = u_h^{n+1} - R_h^{n+1}$, C is a positive constant independent of $\triangle t$ and h.

Proof. We prove this lemma by induction. By the definition of $\bar{x}$ and $\bar{\bar{x}}$, we can see that (4.8) holds for $n = 0$. We assume that (4.8) holds for $1 \le n \le l - 1$. Then $L_n < +\infty$. Now we prove (4.8) for $n = l$.

Letting $\varphi_h = 0$ in (3.12) and using the define of V_h, we can get

$$\begin{aligned} &\left(\frac{3u_h^{l+1} - 4\bar{u}_h^l + \bar{\bar{u}}_h^{l-1}}{2\triangle t}, v_h \right) + \nu a(u_h^{l+1}, v_h) \\ &\quad + \nu_T ((I - P_{L_H})\nabla u_h^{l+1}, (I - P_{L_H})\nabla v_h) = (f^{l+1}, v_h), \quad \forall v_h \in V_h. \end{aligned} \tag{4.9}$$

Subtracting $\left(\frac{3R_h^{l+1}-4\bar{R}_h^l+\bar{\bar{R}}_h^{l-1}}{2\triangle t},v_h\right)+\nu a(R_h^l,v_h)$ from both sides of (4.9), gives

$$\begin{aligned}&\left(\frac{3(u_h^{l+1}-R_h^{l+1})-4(\bar{u}_h^l-\bar{R}_h^l)+(\bar{\bar{u}}_h^{l-1}-\bar{\bar{R}}_h^{l-1})}{2\triangle t},v_h\right)\\&\quad+\nu a(u_h^{l+1}-R_h^{l+1},v_h)+\nu_T((I-P_{L_H})\nabla u_h^{l+1},(I-P_{L_H})\nabla v_h)\\&=(f^l,v_h)-\left(\frac{3R_h^{l+1}-4\bar{R}_h^l+\bar{\bar{R}}_h^{l-1}}{2\triangle t},v_h\right)-\nu a(R_h^{l+1},v_h).\end{aligned}\tag{4.10}$$

Define $\eta^l=u^l-R_h^l$. We can get

$$\begin{aligned}&\left(\frac{3\xi_h^{l+1}-4\xi_h^l+\xi_h^{l-1}}{2\triangle t},v_h\right)+\nu a(\xi_h^{l+1},v_h)+\nu_T((I-P_{L_H})\nabla\xi_h^{l+1},(I-P_{L_H})\nabla v_h)\\
=&-\left(\frac{3u^{l+1}-4\tilde{u}^l+\tilde{\tilde{u}}^{l-1}}{2\triangle t}-\nu\triangle u^{l+1}+\nabla p^{l+1}-f^l,v_h\right)\\
&+\left(\frac{3\eta^{l+1}-4\bar{\eta}^l+\bar{\bar{\eta}}^{l-1}}{2\triangle t},v_h\right)+\left(\frac{4(\bar{u}^l-\tilde{u}^l)-(\bar{\bar{u}}^{l-1}-\tilde{\tilde{u}}^{l-1})}{2\triangle t},v_h\right)\\
&+\left(\frac{4(\bar{\xi}_h^l-\xi_h^l)-(\bar{\bar{\xi}}_h^{l-1}-\xi_h^{l-1})}{2\triangle t},v_h\right)+\nu a(u^{l+1}-R_h^{l+1},v_h)+(\nabla p^{l+1},v_h)\\
&+\nu_T((I-P_{L_H})\nabla\eta_h^{l+1},(I-P_{L_H})\nabla v_h)+\nu_T((I-P_{L_H})\nabla u^{l+1},(I-P_{L_H})\nabla v_h)\\
=&-\left(\frac{3u^{l+1}-4\tilde{u}^l+\tilde{\tilde{u}}^{l-1}}{2\triangle t}-\nu\triangle u^{l+1}+\nabla p^{l+1}-f^l,v_h\right)\\
&+\left(\frac{3\eta^{l+1}-4\bar{\eta}^l+\bar{\bar{\eta}}^{l-1}}{2\triangle t},v_h\right)+\left(\frac{4(\bar{u}^l-\tilde{u}^l)-(\bar{\bar{u}}^{l-1}-\tilde{\tilde{u}}^{l-1})}{2\triangle t},v_h\right)\\
&+\left(\frac{4(\bar{\xi}_h^l-\xi_h^l)-(\bar{\bar{\xi}}_h^{l-1}-\xi_h^{l-1})}{2\triangle t},v_h\right)+\nu a(u^{l+1}-R_h^{l+1},v_h)\\
&+\nu_T((I-P_{L_H})\nabla\eta_h^{l+1},(I-P_{L_H})\nabla v_h)\\
&+\nu_T((I-P_{L_H})\nabla u^{l+1},(I-P_{L_H})\nabla v_h)+d(p^{l+1}-Q_h^{l+1},v_h)\\
=&-\left(\frac{3u^{l+1}-4\tilde{u}^l+\tilde{\tilde{u}}^{l-1}}{2\triangle t}-\nu\triangle u^{l+1}+\nabla p^{l+1}-f^l,v_h\right)\\
&+\left(\frac{3\eta^{l+1}-4\bar{\eta}^l+\bar{\bar{\eta}}^{l-1}}{2\triangle t},v_h\right)+\left(\frac{4(\bar{u}^l-\tilde{u}^l)-(\bar{\bar{u}}^{l-1}-\tilde{\tilde{u}}^{l-1})}{2\triangle t},v_h\right)\\
&+\left(\frac{4(\bar{\xi}_h^l-\xi_h^l)-(\bar{\bar{\xi}}_h^{l-1}-\xi_h^{l-1})}{2\triangle t},v_h\right)+\nu_T((I-P_{L_H})\nabla\eta_h^{l+1},(I-P_{L_H})\nabla v_h)\\
&+\nu_T((I-P_{L_H})\nabla u^{l+1},(I-P_{L_H})\nabla v_h).\end{aligned}\tag{4.11}$$

By the definition of $\bar{x}$ and $\tilde{x}$, we arrive at $\bar{x}(x,t_l)-\tilde{x}(x,t_{l-1})=(u^{l*}-u_h^{l*})\triangle t$. Using the Taylor formula yields

$$\begin{aligned}|\bar{u}^l-\tilde{u}^l|&=|u^l(\tilde{x})-u^l(\bar{x})|\le\triangle t\|\nabla u^l\|_\infty|(u^{l*}-u_h^{l*})|\\&\le\triangle t\|\nabla u^l\|_\infty\Big(|(u_h^{l*}-R_h^{l*})|+|R_h^{l*}-u^{l*}|\Big).\end{aligned}$$

Therefore, we get

$$\frac{1}{\triangle t}\|\bar{u}^l-\tilde{u}^l\|_0 \le \|\nabla u^l\|_\infty\Big(\|u^{l*}-R_h^{l*}\|_0+\|R_h^{l*}-u_h^{1,l*}\|_0\Big)$$
$$\le C\Big(h^{k+1}+\|\xi_h^l\|_0+\|\xi_h^{l-1}\|_0\Big). \tag{4.12}$$

Similarly, we can get the estimate

$$\frac{1}{\triangle t}\|\bar{\bar{u}}^{l-1}-\tilde{\tilde{u}}^{l-1}\|_0 \le C\Big(h^{k+1}+\|\xi_h^l\|_0+\|\xi_h^{l-1}\|_0\Big). \tag{4.13}$$

Now, we estimate the bound of $\|\frac{3\eta^{l+1}-4\bar{\eta}^l+\bar{\bar{\eta}}^{l-1}}{2\triangle t}\|_0$. Note that

$$\frac{3\eta^{l+1}-4\bar{\eta}^l+\bar{\bar{\eta}}^{l-1}}{2\triangle t}$$
$$=\frac{3(\eta^{l+1}-\eta^l)-(\eta^l-\eta^{l-1})}{2\triangle t}+\frac{4(\eta^l-\bar{\eta}^l)+(\bar{\bar{\eta}}^{l-1}-\eta^{l-1})}{2\triangle t}.$$

By the Taylor's formula, we have

$$\|\eta^{l+1}-\eta^l\|_0=\Big(\int_\Omega(\eta^{l+1}-\eta^l)^2dx\Big)^{\frac{1}{2}}=\left(\int_\Omega\left(\triangle t\frac{\partial\eta^l}{\partial t}+\mathbb{O}(\triangle t^2)\right)^2dx\right)^{\frac{1}{2}}$$
$$\le C\triangle t\left\|\frac{\partial\eta^l}{\partial t}\right\|_0. \tag{4.14}$$

We estimate $\|\eta^l-\eta^{l-1}\|_0$ in the same way

$$\|\eta^l-\eta^{l-1}\|_0 \quad\le\quad C\triangle t\left\|\frac{\partial\eta^{l-1}}{\partial t}\right\|_0. \tag{4.15}$$

By the definition of $\bar{\mathcal{X}}_x^l(t_{l-1})$, we get

$$J(\bar{\mathcal{X}}_x^l(t_{l-1}))=\begin{pmatrix}1-\partial_x u_{h1}^{l*}\triangle t & -\partial_y u_{h1}^{l*}\triangle t\\ -\partial_x u_{h2}^{l*}\triangle t & 1-\partial_y u_{h2}^{n*}\triangle t\end{pmatrix}. \tag{4.16}$$

Hence,

$$\det J(\bar{\mathcal{X}}_x^l(t_{l-1}))=1+\mathcal{O}(\triangle t). \tag{4.17}$$

Then, we obtain

$$\|\eta^l-\bar{\eta}^l\|_{-1}=\sup_{v\in V}\left[\|\nabla v\|_0^{-1}(\eta^l-\bar{\eta}^l,v)\right]$$
$$=\sup_{v\in V}\left[\|\nabla v\|_0^{-1}\left(\int_\Omega\eta^l(x)v(x)dx\ -\int_\Omega\eta^l(z)v(\hat{\mathcal{X}}_x^l(t_l)^{-1})(1+\mathcal{O}(\triangle t))dz\right)\right]$$
$$\le\sup_{v\in V}\left(\|\nabla v\|_0^{-1}\int_\Omega\eta^l(x)(v(x)-v(\hat{\mathcal{X}}_x^l(t_l)^{-1}))dx\right)$$
$$+\sup_{v\in V}\left(C\triangle t^2\|\nabla v\|_0^{-1}\int_\Omega\eta^l(z)v(\hat{\mathcal{X}}_x^l(t_l)^{-1}))dz\right).$$

Let $G(x) = x - \bar{\mathcal{X}}_x^l(t_l)^{-1}$. Then $|G(x)| \le C\triangle t$, and

$$\|v(x) - v(\bar{\mathcal{X}}_x^l(t_l)^{-1})\|_0^2 \le \int_\Omega \left(\int_{t_n-1}^{t_l} \frac{d}{dt} v(\hat{\mathcal{X}}_x^l(t)^{-1})dt\right)^2 dx$$
$$\le C\triangle t^2 \|\nabla v\|_0^2.$$

Similarly, we have

$$\|v(\bar{\mathcal{X}}_x^l(t_l)^{-1})\|_0 \le \|v\|_0^2(1 + C\triangle t).$$

Then, we can deduce

$$\|\eta^l - \bar{\eta}^l\|_{-1} \le C\triangle t \|\eta^l\|_0. \tag{4.18}$$

By (4.14) and (4.18), we can get

$$\left\|\frac{\eta^l - \bar{\eta}^l}{\triangle t}\right\|_{-1} \le Ch^{k+1}\|u_h^{l*}\|_\infty. \tag{4.19}$$

Similarly, we get

$$\left\|\frac{\eta^{l-1} - \bar{\bar{\eta}}^{l-1}}{\triangle t}\right\|_{-1} \le Ch^{k+1}\|u_h^{l*}\|_\infty. \tag{4.20}$$

By (4.14), (4.15), (4.19) and (4.20), we obtain

$$\left\|\frac{3\eta^{l+1} - 4\bar{\eta}^l + \bar{\bar{\eta}}^{l-1}}{2\triangle t}\right\|_{-1} \le Ch^{k+1}\|u_h^{l*}\|_\infty. \tag{4.21}$$

Using the similar method, we can obtain

$$\left\|\frac{4(\bar{\xi}_h^l - \xi_h^l) - (\bar{\bar{\xi}}_h^{l-1} - \xi_h^{l-1})}{2\triangle t}\right\|_{-1} \le C\Big(\|\xi_h^l\|_0 + \|\xi_h^{l-1}\|_0\Big). \tag{4.22}$$

Here, we define $\delta\xi_h^{l+1} = \xi_h^{l+1} - \xi_h^l$. Letting $v_h = \delta\xi_h^{l+1}$ in (4.11), we get

$$\begin{aligned}
&\left(\frac{3}{2\triangle t}\delta\xi_h^{l+1} - \frac{1}{2\triangle t}\delta\xi_h^l, \delta\xi_h^{l+1}\right) + \frac{\nu + \nu_{add}}{2}a(\xi_h^{l+1}, \xi_h^{l+1}) - \frac{\nu + \nu_{add}}{2}a(\xi_h^l, \xi_h^l)\\
=& -\left(\tilde{e}(x, l+1), \delta\xi_h^{l+1}\right) + \left(\frac{3\eta^{l+1} - 4\bar{\eta}^l + \bar{\bar{\eta}}^{l-1}}{2\triangle t}, \delta\xi_h^{l+1}\right)\\
&+ \left(\frac{4(\bar{u}^l - \tilde{u}^l) - (\bar{\bar{u}}^{l-1} - \tilde{\tilde{u}}^{l-1})}{2\triangle t}, \delta\xi_h^{l+1}\right)\\
&+ \left(\frac{4(\bar{\xi}_h^l - \xi_h^l) - (\bar{\bar{\xi}}_h^{l-1} - \xi_h^{l-1})}{2\triangle t}, \delta\xi_h^{l+1}\right)\\
&+\nu_T((I - P_{L_H})\nabla\eta_h^{l+1}, (I - P_{L_H})\delta\xi_h^{l+1})\\
&+\nu_T((I - P_{L_H})\nabla u^{l+1}, (I - P_{L_H})\delta\xi_h^{l+1}).
\end{aligned}$$

Summing over the above equality from $i=2$ to l, we can get

$$\begin{aligned}
&\sum_{i=1}^{l}\left(\frac{1}{\triangle t}\delta\xi_h^{i+1},\delta\xi_h^{i+1}\right)+\frac{\nu+\nu_{add}}{2}a(\xi_h^{l+1},\xi_h^{l+1})\\
=&\frac{\nu+\nu_{add}}{2}a(\xi_h^1,\xi_h^1)+\sum_{i=2}^{n}\left(\tilde{e}(x,i+1)-\tilde{e}(x,i),\xi_h^{i+1}\right)\\
&+\sum_{i=2}^{l}\left(\frac{3\eta^{i+1}-4\bar{\eta}^i+\bar{\bar{\eta}}^{i-1}}{2\triangle t}-\frac{3\eta^i-4\bar{\eta}^{i-1}+\bar{\bar{\eta}}^{i-2}}{2\triangle t},\xi_h^{i+1}\right)\\
&+\sum_{i=2}^{l}\left(\frac{4(\bar{u}^i-\tilde{u}^i)-(\bar{\bar{u}}^{i-1}-\tilde{\tilde{u}}^{i-1})}{2\triangle t}-\frac{4(\bar{u}^{i-1}-\tilde{u}^{i-1})-(\bar{\bar{u}}^{i-2}-\tilde{\tilde{u}}^{i-2})}{2\triangle t},\xi_h^{i+1}\right)\\
&+\sum_{i=2}^{l}\left(\frac{4(\bar{\xi}_h^i-\xi_h^i)-(\bar{\bar{\xi}}_h^{i-1}-\xi_h^{i-1})}{2\triangle t}-\frac{4(\bar{\xi}_h^{i-1}-\xi_h^{i-1})-(\bar{\bar{\xi}}_h^{i-2}-\xi_h^{i-2})}{2\triangle t},\xi_h^{i+1}\right)\\
&+\sum_{i=2}^{l}\nu_T((I-P_{L_H})\nabla\eta_h^{i+1}-(I-P_{L_H})\nabla\eta_h^i,(I-P_{L_H})\xi_h^{i+1})\\
&+\sum_{i=2}^{l}\nu_T((I-P_{L_H})\nabla u^{i+1}-(I-P_{L_H})\nabla u^i,(I-P_{L_H})\xi_h^{i+1}). \qquad (4.23)
\end{aligned}$$

Setting $v_h=\xi_h^{l+1}$ in (4.11), we obtain

$$\begin{aligned}
&\left(\frac{3}{2\triangle t}\delta\xi_h^{l+1}-\frac{1}{2\triangle t}\delta\xi_h^l,\xi_h^{l+1}\right)+\frac{\nu+\nu_{add}}{2}a(\xi_h^{l+1},\xi_h^{l+1})\\
=&-\left(\tilde{e}(x,l+1),\xi_h^{l+1}\right)+\left(\frac{3\eta^{l+1}-4\bar{\eta}^l+\bar{\bar{\eta}}^{l-1}}{2\triangle t},\xi_h^{l+1}\right)\\
&+\left(\frac{4(\bar{u}^l-\tilde{u}^l)-(\bar{\bar{u}}^{l-1}-\tilde{\tilde{u}}^{l-1})}{2\triangle t},\xi_h^{l+1}\right)+\left(\frac{4(\bar{\xi}_h^l-\xi_h^l)-(\bar{\bar{\xi}}_h^{l-1}-\xi_h^{l-1})}{2\triangle t},\xi_h^{l+1}\right)\\
&+\nu_T((I-P_{L_H})\nabla\eta_h^{l+1},(I-P_{L_H})\xi_h^{l+1})+\nu_T((I-P_{L_H})\nabla u^{l+1},(I-P_{L_H})\xi_h^{l+1}).
\end{aligned}$$

By $\xi_h^{l+1}=\delta\xi_h^{l+1}+\delta\xi_h^l+\xi_h^{l-1}$ and Young's inequality, we can get

$$\begin{aligned}
&\frac{3}{4\triangle t}\left[\left(\xi_h^{l+1},\xi_h^{l+1}\right)-\left(\xi_h^l,\xi_h^l\right)\right]+\frac{\nu+\nu_{add}}{2}a(\xi_h^{l+1},\xi_h^{l+1})\\
\le&\frac{1}{4\triangle t}\left(\delta\xi_h^{l+1},\delta\xi_h^{l+1}\right)+\frac{3}{4\triangle t}\left(\delta\xi_h^l,\delta\xi_h^l\right)+\frac{1}{4\triangle t}\left[\left(\xi_h^l,\xi_h^l\right)-\left(\xi_h^{l-1},\xi_h^{l-1}\right)\right]\\
&-\left(\tilde{e}(x,l+1),\xi_h^{l+1}\right)+\left(\frac{3\eta^{l+1}-4\bar{\eta}^l+\bar{\bar{\eta}}^{l-1}}{2\triangle t},\xi_h^{l+1}\right)\\
&+\left(\frac{4(\bar{u}^l-\tilde{u}^l)-(\bar{\bar{u}}^{l-1}-\tilde{\tilde{u}}^{l-1})}{2\triangle t},\xi_h^{l+1}\right)+\left(\frac{4(\bar{\xi}_h^l-\xi_h^l)-(\bar{\bar{\xi}}_h^{l-1}-\xi_h^{l-1})}{2\triangle t},\xi_h^{l+1}\right)\\
&+\nu_T((I-P_{L_H})\nabla\eta_h^{l+1},(I-P_{L_H})\xi_h^{l+1})\\
&+\nu_T((I-P_{L_H})\nabla u^{l+1},(I-P_{L_H})\xi_h^{l+1}).
\end{aligned}$$

Using the Cauchy-Schwarz and Young's inequality, we can deduce

$$
\begin{aligned}
&\frac{3}{4}\frac{\|\xi_h^{l+1}\|_0^2-\|\xi_h^l\|_0^2}{\triangle t}+(\nu+\nu_{add})\|\nabla\xi_h^{l+1}\|_0^2\\
\le&\frac{1}{4\triangle t}\left(\delta\xi_h^{l+1},\delta\xi_h^{l+1}\right)+\frac{3}{4\triangle t}\left(\delta\xi_h^{l},\delta\xi_h^{l}\right)+\frac{1}{4\triangle t}\left[\left(\xi_h^{l},\xi_h^{l}\right)-\left(\xi_h^{l-1},\xi_h^{l-1}\right)\right]\\
&+C\left\|\frac{3u^{l+1}-4\tilde{u}^l+\tilde{\tilde{u}}^{l-1}}{2\triangle t}-\nu\triangle u^{l+1}+\nabla p^{l+1}-f^{l+1}\right\|_0\|\nabla\xi_h^{l+1}\|_0\\
&+\left\|\frac{3\eta^{l+1}-4\bar{\eta}^l+\bar{\bar{\eta}}^{l-1}}{2\triangle t}\right\|_{-1}\|\nabla\xi_h^{l+1}\|_0+\left\|\frac{4(\bar{u}^l-\tilde{u}^l)-(\bar{\bar{u}}^{l-1}-\tilde{\tilde{u}}^{l-1})}{2\triangle t}\right\|_{-1}\|\nabla\xi_h^{l+1}\|_0\\
&+\left\|\frac{4(\bar{\xi}_h^l-\xi_h^l)-(\bar{\bar{\xi}}_h^{l-1}-\xi_h^{l-1})}{2\triangle t}\right\|_{-1}\|\nabla\xi_h^{l+1}\|_0\\
&+\nu_{add}\left\|\nabla\eta_h^{l+1}\right\|_0\left\|\nabla\xi_h^{l+1}\right\|_0+\nu_T\left\|((I-P_{L_H})\nabla u^{l+1}\right\|_0\left\|(I-P_{L_H})\nabla\xi_h^{l+1}\right\|_0\\
\le&\frac{1}{4\triangle t}\left(\delta\xi_h^{l+1},\delta\xi_h^{l+1}\right)+\frac{3}{4\triangle t}\left(\delta\xi_h^{l},\delta\xi_h^{l}\right)+\frac{1}{4\triangle t}\left[\left(\xi_h^{l},\xi_h^{l}\right)-\left(\xi_h^{l-1},\xi_h^{l-1}\right)\right]\\
&+C\left\|\frac{3u^{l+1}-4\tilde{u}^l+\tilde{\tilde{u}}^{l-1}}{2\triangle t}-\nu\triangle u^{l+1}+\nabla p^{l+1}-f^{l+1}\right\|_0^2\\
&+C\left\|\frac{3\eta^{l+1}-4\bar{\eta}^l+\bar{\bar{\eta}}^{l-1}}{2\triangle t}\right\|_{-1}^2+C\left\|\frac{4(\bar{u}^l-\tilde{u}^l)-(\bar{\bar{u}}^{l-1}-\tilde{\tilde{u}}^{l-1})}{2\triangle t}\right\|_{-1}^2\\
&+C\left\|\frac{4(\bar{\xi}_h^l-\xi_h^l)-(\bar{\bar{\xi}}_h^{l-1}-\xi_h^{l-1})}{2\triangle t}\right\|_{-1}^2+C\nu_{add}\left\|\nabla\eta_h^{l+1}\right\|_0^2\\
&+C\nu_T\left\|((I-P_{L_H})\nabla u^{l+1}\right\|_0^2+\frac{\nu+\nu_{add}}{2}\left\|\nabla\xi_h^{l+1}\right\|_0.
\end{aligned}
$$

Using (4.3), (4.12), (4.19) and (4.22) yields

$$
\begin{aligned}
&\frac{\|\xi_h^{l+1}\|_0^2-\|\xi_h^l\|_0^2}{\triangle t}+\frac{\nu+\nu_{add}}{2}\|\nabla\xi_h^{l+1}\|_0^2\\
\le&\frac{1}{4\triangle t}\Big(\delta\xi_h^{l+1},\delta\xi_h^{l+1}\Big)+\frac{3}{4\triangle t}\Big(\delta\xi_h^{l},\delta\xi_h^{l}\Big)+\frac{1}{4\triangle t}\Big[\Big(\xi_h^{l},\xi_h^{l}\Big)-\Big(\xi_h^{l-1},\xi_h^{l-1}\Big)\Big]\\
&+C\Big(\triangle t^4+h^{2k+2}+\nu_{add}h^{2k}\Big)+C\nu_T\triangle t\sum_{i=1}^{l+1}\|(I-P_{L_H})\nabla u^{i+1}\|_0^2. \qquad (4.24)
\end{aligned}
$$

Summing inequality (4.24) from $i=2$ to n, we obtain

$$
\begin{aligned}
&\|\xi_h^{l+1}\|_0^2+\frac{\nu+\nu_{add}}{2}\triangle t\sum_{i=1}^{l+1}\|\nabla\xi_h^i\|_0^2\\
\le&\, C(\xi_h^1,\xi_h^1)+\frac{1}{3}(\xi_h^l,\xi_h^l)+\frac{4}{3}\sum_{i=1}^{l}\left(\delta\xi_h^i,\delta\xi_h^i\right)\\
&+C\left(\triangle t^4+h^{2k+2}+\nu_{add}h^{2k}+\nu_T\triangle t\sum_{i=1}^{l+1}\|(I-P_{L_H})\nabla u^{i+1}\|_0^2\right). \qquad (4.25)
\end{aligned}
$$

By the coefficient of the second term on the right hand side of (4.25) is $\frac{1}{3}$, this term can be ignored (using a recursion argument). Using (4.3), (4.12), (4.19), (4.22) and (4.23), we can deduce

$$\begin{aligned}
&\|\xi_h^{l+1}\|_0^2 + \frac{\nu+\nu_{add}}{2}\triangle t\sum_{i=1}^{l+1}\|\nabla\xi_h^i\|_0^2 \\
\le\ & C\triangle t\sum_{i=1}^{l}\|\xi_h^i\|_0^2 + C\Big(\triangle t^4 + h^{2k+2} + \nu_{add}h^{2k}\Big) \\
&+C\nu_T\triangle t\sum_{i=1}^{l+1}\|(I-P_{L_H})\nabla u^{i+1}\|_0^2. \qquad (4.26)
\end{aligned}$$

As application of Gronwall's Lemma yields

$$\begin{aligned}
&\|\xi_h^{l+1}\|_0^2 + \frac{\nu+\nu_{add}}{2}\triangle t\sum_{i=1}^{l+1}\|\nabla\xi_h^i\|_0^2 \\
\le\ & C\exp(CT)\Big(\triangle t^4 + h^{2k+2} + \nu_{add}h^{2k} + \nu_T\triangle t\sum_{i=1}^{n+1}\|(I-P_{L_H})\nabla u^{i+1}\|_0^2\Big).
\end{aligned}$$

It follows from the triangle inequality that

$$\|u_h^{l+1}\|_\infty \le \|u_h^{l+1} - R_h^{l+1}\|_\infty + \|R_h^{l+1}\|_\infty.$$

Using the inverse inequality, $\|v_h\|_\infty \le Ch^{-1}\|\nabla v_h\|_0$ (see [5]), we can get

$$\|u_h^{l+1}\|_\infty \le Ch^{-1}\|\nabla(u_h^{l+1} - R_h^{l+1})\|_0 + \|R_h^{l+1}\|_\infty.$$

This, together with (4.26) and Lemma 4.4, yields the defined results. □

Remark 4.1 Define $\bar{\mathcal{X}}_x^n(t) = x - (t_n - t)u_h^{n*}, \forall t\in[t^{n-2}, t^n], 2\le n\le N$. Since X_h is a subset of $W^{1,\infty}(\Omega)$, under the condition (4.7) on the time step it is an easy matter to verify that this mapping has a positive Jacobian, since u_h^n vanishes on $\partial\Omega$; this mapping is one-to-one from Ω onto Ω and is a change of variables. This yields for any positive function ϕ on Ω the estimate (please see [5] for detail)

$$\int_\Omega \phi(\bar{\mathcal{X}}_h^n(t))dx \le C\int_\Omega \phi(x)dx.$$

Theorem 4.1. *Let u_h^n be defined by* (3.10) *and u be the solution of* (2.1)*. If $\triangle t$ is sufficient small, for all $1\le n\le N-1$ we have*

$$\begin{aligned}
&\|u^{n+1} - u_h^{n+1}\|_0^2 \\
\le\ & C\exp(CT)\Big(\triangle t^4 + h^{2k+2} + \nu_{add}h^{2k} + \nu_T\triangle t\sum_{i=1}^{n+1}\|(I-P_{L_H})\nabla u^i\|_0^2\Big), \\
&\nu\triangle t\sum_{i=1}^{n+1}\|\nabla(u^i - u_h^i)\|_0^2 \\
\le\ & C\exp(CT)\Big(\triangle t^4 + h^{2k+2} + \nu_{add}h^{2k} + \nu_T\triangle t\sum_{i=1}^{n+1}\|(I-P_{L_H})\nabla u^i\|_0^2\Big) + Ch^{2k}.
\end{aligned}$$

Proof. Using the triangle inequality, (4.5) and (4.8b), we can get this theorem. □

Corollary 4.1. *Under the assumptions of Lemma* 4.4*, Remark* 3.2*, the regularity assumption of* $(u,p)\in(H^3(\Omega)^2\cap X, H^2(\Omega)\cap M), \forall t\in(0,T]$ *and the assumption of* ν_T*, for all* $1\le n\le N-1$ *we have the following error analysis*

$$\|u^{n+1}-u_h^{n+1}\|_0^2 \le C\exp(CT)\Big(\triangle t^4 + h^{2k+2}\Big),$$

$$\nu\triangle t\sum_{i=1}^{n+1}\|\nabla(u^i-u_h^i)\|_0^2 \le C\exp(CT)\Big(\triangle t^4 + h^{2k}\Big).$$

The following theorem on the pressure is a consequence of the previous theorem on the velocity.

Theorem 4.2. *Under the assumptions of Lemma* 4.4*, for all* $1\le n\le N-1$ *we have*

$$\left(\sum_{i=1}^{n+1}\triangle t\|p^i-p_h^i\|_0^2\right)^{1/2} \le C\left(\triangle t^2 + h^k + \nu_T\triangle t\sum_{i=1}^{n+1}\|(I-P_{L_H})\nabla u^i\|_0^2\right),$$

where C *is a positive constant.*

Proof. Multiplying (4.2) by $v_h\in X_h$ and subtracting the resulting form (3.12) with $\varphi_h=0$, we obtain

$$\begin{aligned}
&d(Q_h^{n+1}-p_h^{n+1},v_h)\\
&= -(\bar{e}(x,n),v_h) + \left(\frac{3(u_h^{n+1}-u^{n+1}) - 4(\bar{u}_h^n-\tilde{u}^n) + (\bar{\bar{u}}_h^{n-1}-\tilde{\tilde{u}}^{n-1})}{2\triangle t}, v_h\right)\\
&\quad + d(Q_h^{n+1}-p^{n+1},v_h) + \nu a(u_h^{n+1}-u^{n+1},v_h) + \nu_T((I-P_{L_h})\nabla u_h^{n+1},(I-P_{L_H})\nabla v_h).
\end{aligned}$$

By the inf-sup condition and Cauchy-Schwarz inequality, we can get

$$\begin{aligned}
&\|Q_h^{n+1}-p_h^{n+1}\|_0\\
&\le C\left[\|\bar{e}(x,n)\|_0 + \left\|\frac{u^{n+1}-u_h^{n+1}}{\triangle t}\right\|_0 + \left\|\frac{\bar{u}_h^n-\tilde{u}^n}{\triangle t}\right\|_0 + \left\|\frac{\bar{\bar{u}}_h^{n-1}-\tilde{\tilde{u}}^{n-1}}{\triangle t}\right\|_0\right]\\
&\quad + C\|Q_h^{n+1}-p^{n+1}\|_0 + \nu\|\nabla(u_h^{n+1}-u^{n+1})\|_0
\end{aligned} \tag{4.27}$$

Using (4.3), (4.12) and (4.27), we can get

$$\left(\sum_{i=1}^{n+1}\triangle t\|Q_h^i-p_h^i\|_0^2\right)^{1/2} \le C(\triangle t^2 + h^k + \nu_T\triangle t\sum_{i=1}^{n+1}\|(I-P_{L_H})\nabla u^i\|_0^2).$$

By the triangle inequality, we have

$$\begin{aligned}
\left(\sum_{i=1}^{n+1}\triangle t\|p^i-p_h^i\|_0^2\right)^{1/2} &\le \left(\sum_{i=1}^{n+1}\triangle t\|Q_h^i-p_h^i\|_0^2\right)^{1/2} + \left(\sum_{i=1}^{n+1}\triangle t\|Q_h^i-p^i\|_0^2\right)^{1/2}\\
&\le C\Big(\triangle t^2 + h^k + \nu_T\triangle t\sum_{i=1}^{n+1}\|(I-P_{L_H})\nabla u^i\|_0^2\Big).
\end{aligned} \tag{4.28}$$

Therefore, we finish the proof. □

Corollary 4.2. *Under the assumptions of Lemma* 4.4*, Remark* 3.2*, the regularity assumption of* $(u,p) \in (H^3(\Omega)^2 \cap X, H^2(\Omega) \cap M), \forall t \in (0,T]$ *and the assumption of* ν_T*, we have the following error analysis for* p

$$\left(\sum_{i=1}^{n+1} \triangle t \|p^i - p_h^i\|_0^2\right)^{1/2} \leq C(\triangle t^2 + h^k). \tag{4.29}$$

5. Numerical Results

5.1. A problem with analytical solution

In this subsection, we present some numerical results of the Navier-Stokes problems with the analytical solution

$$\begin{aligned}
u_1 &= 10x^2(x-1)^2 y(y-1)(2y-1)\exp(-2\pi^2 t\nu),\\
u_2 &= -10x(x-1)(2x-1)y^2(y-1)^2\exp(-2\pi^2 t\nu),\\
p &= 20(2x-1)(2y-1)\exp(-4\pi^2 t\nu).
\end{aligned}$$

The boundary and initial condition in (2.1) are set equal to the analytical solution and f is given by evaluating the momentum equation of problem (2.1) for the analytical solution.

We choose $\triangle t = 0.001$, $T = 1$ and $Re = 2000$. We present the numerical results with different h respectively and the finite elements are $P_2 - P_1$ element space. The numerical results are shown in Table 5.1.

The numerical results in Table 5.1 show that the convergence rates are $\mathcal{O}(h^3)$ of the L^2-norm for u, $\mathcal{O}(h^2)$ of the H^1-semi norm for u and $\mathcal{O}(h^2)$ of the L^2-norm for p, which agrees very well with our theoretical results by using $P_2 - P_1$ finite element spaces.

Table 5.1: The numerical results at $T = 1$ with $\triangle t = 0.001, Re = 2000, \sigma = 0.4h$.

$1/h$	$\frac{\\|u-u_h\\|_0}{\\|u\\|_0}$	$\frac{\\|\nabla(u-u_h)\\|_0}{\\|u\\|_0}$	$\frac{\\|p-p_h\\|_0}{\\|p\\|_0}$	u_{L_2} rate	u_{H_1} rate	P_{L_2} rate
10	0.002590	0.03066	0.007745	–	–	–
20	0.0003127	0.007478	0.001936	3.049	2.035	2.000
30	9.193×10^{-5}	0.003299	8.606×10^{-4}	3.019	2.018	1.999
40	3.887×10^{-5}	0.001851	4.841×10^{-4}	2.992	2.009	1.999
50	2.027×10^{-5}	0.001183	3.098×10^{-4}	2.915	2.005	1.999
60	1.236×10^{-5}	8.211×10^{-4}	2.151×10^{-4}	2.715	2.003	1.999

5.2. The lid driven cavity problem

In this section we show the numerical results of lid driven cavity problem. The two-demensional lid driven was formulated as in $\Omega = (0,1)^2$, the boundary conditions are $u_1 = 1, u_2 = 0$ on the top lid and $u_1 = 0, u_2 = 0$ on the other lids. In a former work [3,17,20], it was suggested that the first Hopf bifurcation occurs around Reynolds number Re = 8000. In this numerical experiments, $h = \frac{1}{60}$, $\triangle t = 0.01$, $\nu_T = \delta h^2 \|\nabla u_h\|_0$, $\delta = 0.5$ are chosen. We choose the Taylor-Hood element and $L_H = \{\mathbb{L} \in (L^2(\Omega))^{2\times 2},\ \mathbb{L}|_K \in P_{1dc}^{2\times 2}\ ,\forall K \in \Im_h\}$, where P_{1dc} is the piecewise linear discontinuous finite element space.

Firstly, we choose $Re = 5000$ and 7500, which are good choices as there are some comparisons available in the literature and as the steady solutions are still stable but not too far from the first

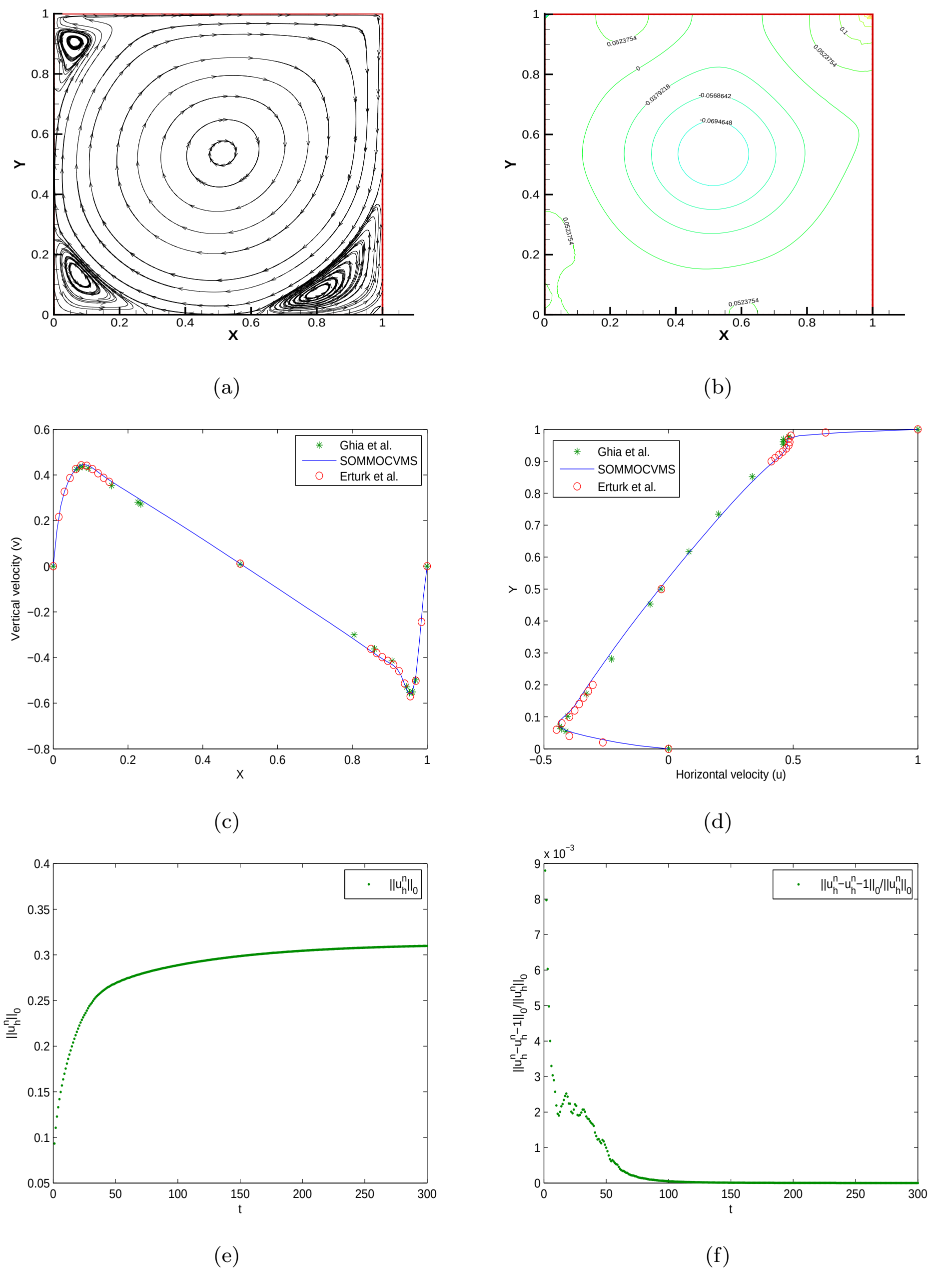

Fig. 5.1. The numerical results for $Re = 5000$ with $\nu_T = \delta h^2 \|\nabla u_h\|_0$. (a) The numerical streamline at $t = 300$; (b) The numerical pressure contours at $t = 300$; (c) The computed u-velocity profiles along a vertical line passing through the geometric center of the cavity at $t = 300$; (d) The computed v-velocity profiles along a horizontal line passing through the geometric center at $t = 300$; (e) Evolution of $||u_h^n||_0$ in time; (f) Evolution of the error $\|u_h^n - u_h^{n-1}\|_0 / \|u_h^n\|_0$ in time.

Hopf bifurcation. Figs. 5.1 and 5.2 gives the numerical results of $Re = 5000$ and $Re = 7500$, respectively ((a) the numerical streamline at $t = 300$; (b) the numerical pressure contours at

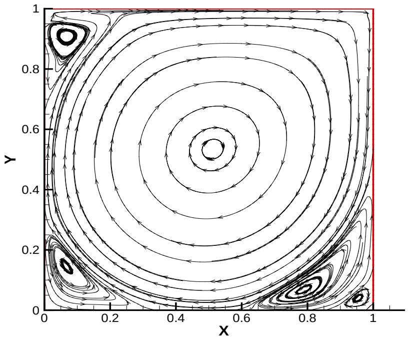

(a)

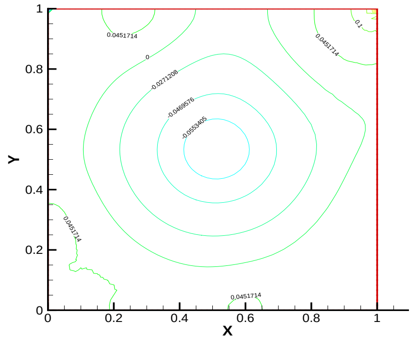

(b)

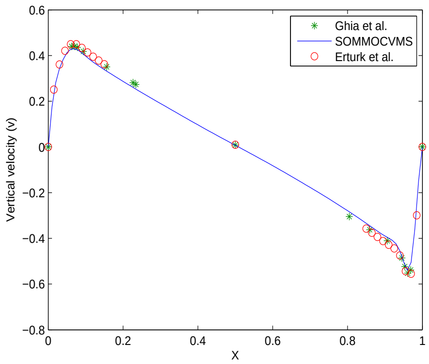

(c)

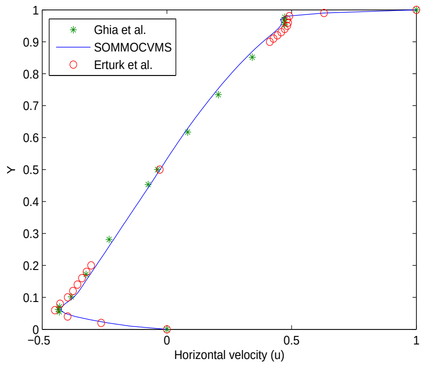

(d)

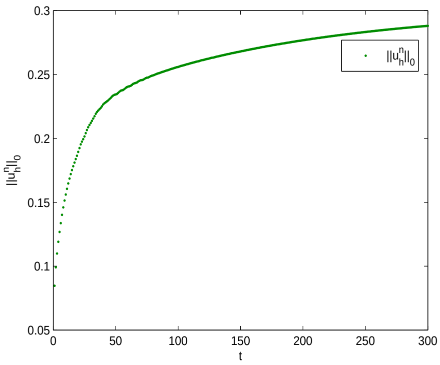

(e)

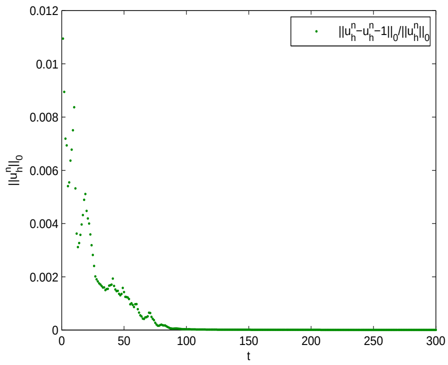

(f)

Fig. 5.2. Same as Fig. 5.1, except for $R_e = 7500$.

$t = 300$; (c) the computed u-velocity profiles along a vertical line passing through the geometric center of the cavity at $t = 300$; (d) the computed v-velocity profiles along a horizontal line passing through the geometric center of the cavity at $t = 300$; (e)the evolution of $||u_h^n||_0$ in time and (f) the evolution of the error $\|u_h^n - u_h^{n-1}\|_0/\|u_h^n\|_0$ in time).

From the numerical results, we can see that the kinetic energy reaches a stable state, the error $\|u_h^n - u_h^{n-1}\|_0/\|u_h^n\|_0$ changes very small. It means that a steady solution of the time-dependent

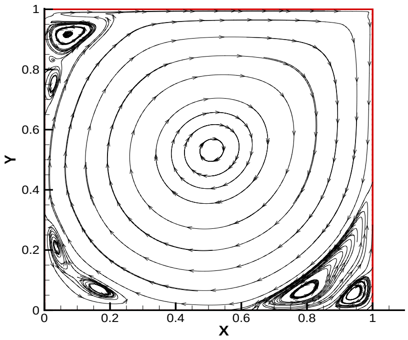

(a) t=325.

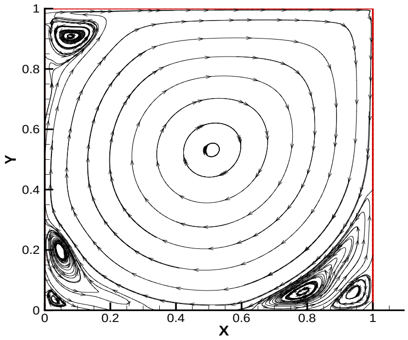

(b) t=350.

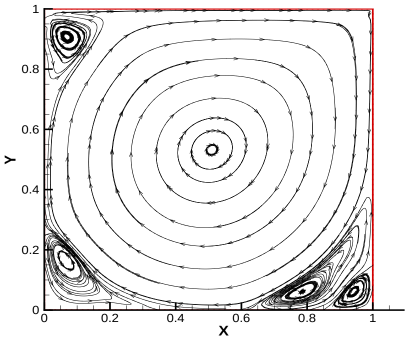

(c) t=375

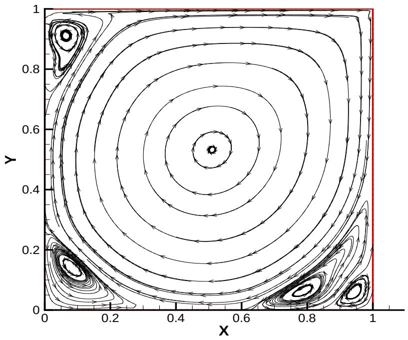

(d) t=400

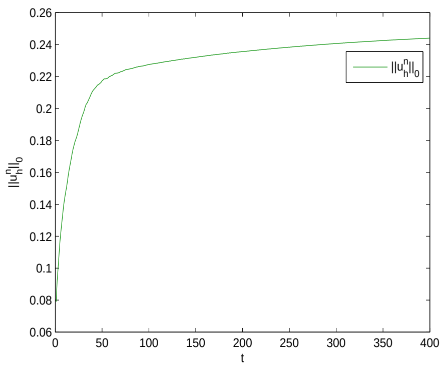

(e)

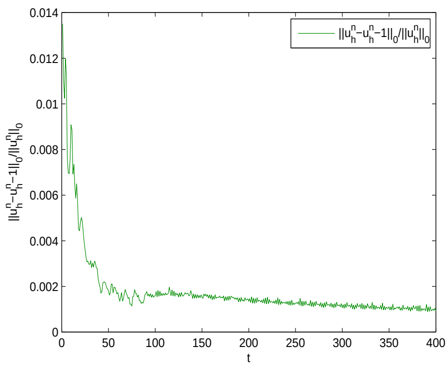

(f)

Fig. 5.3. The numerical streamlines for $Re = 10000$ with $\nu_T = \delta h^2 \|u_h^n\|_0$ at different time (a-d) and the evolution of $||u_h^n||_0$ in time (e) and evolution of the error $\|u_h^n - u_h^{n-1}\|_0 / \|u_h^n\|_0$ (f) for $Re = 10000$ with $\nu_T = \delta h^2 \|u_h^n\|_0$.

Navier-Stokes equations was obtained. u-velocity profiles along a vertical line passing through the geometric center of the cavity and v-velocity profiles along a horizontal line passing through the geometric center of the cavity agree very well with the results of the steady Navier-Stokes equations given by Erturk et al. [17].

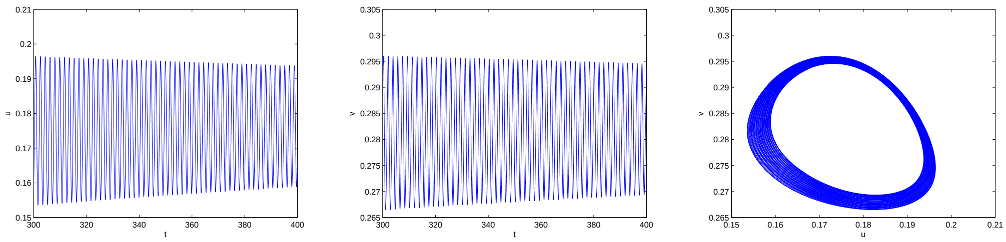

(a) (b) (c)

Fig. 5.4. u-velocity history (a), v-velocity history (b) and the phase portrait (c), at monitoring point $(1/8, 13/16)$ for $Re = 10000$ with $\nu_T = \delta h^2 \|u_h^n\|_0$ from $t = 200$ to $t = 300$.

At last, we show some numerical results for $Re = 10000$, which is probably the most famous value and for quite a long time as the question was to known if the steady solution was stable or not for this Renolds number. Bruneau and Saad [7] shown that the steady solution is not stable and the first Hopf bifurcation occurs around $Re = 8000$. Fig. 5.3 presents the streamlines at different time $((a) \sim (d))$. Fig. 5.3 also shows the evolution of $||u_h^n||_0$ in time (e) and evolution of the error $\|u_h^n - u_h^{n-1}\|_0 / \|u_h^n\|_0$ in time (f). We choose a monitoring points $(1/8, 13/16)$ to show the properties of the solutions. Fig. 5.4 shows u-velocity history (a), v-velocity history (b) and the phase portrait (c) at the monitoring point. It shows that the stable solution is quasi-periodic and has small variations in the amplitude of the time evolution at the monitoring point. And the phase portraits show that the variations in amplitude yield a solution which is quasi-periodic. We can see that the kinetic energy dose not change as the time change long enough and the error dose not change small. The results are very close the those shown by [7]. The numerical experiments confirm our theoretical analysis and demonstrate the efficiency of the second order MCVMS finite element method.

Acknowledgments. The authors would like to thank the editor and the referees for their valuable comments, which led to the improvement of this paper. This work is supported by the NSF of China (No. 11271298, No. 11226306 and No. 11001216) and the Doctoral Foundation of Henan Polytechnic University (No. B2012-56).

References

[1] A. Allievi, R. Bermejo, Finite element modified method of characteristics for the Navier-Stokes equations, *Int. J. Numer. Meth. Fluids*, **32** (2000), 439-464.

[2] T. Arbogast, M.F. Wheeler, A characteristics-mixed finite element method for advection-dominated transport problems, *SIAM J. Numer. Anal.*, **32** (2) (1995), 404-424.

[3] G. Bruneaua, C. Jouron, An efficient scheme for solving steady incompressible Navier-Stokes equations, *J. Comput. Phys.*, **89**(2) (1990), 389-413.

[4] K. Boukir, Y. Maday, B. MéTivet, A high order characteristics method for the incompressible Navier-Stokes equations, *Comput. Methods Appl. Mech. Engrg.*, **116** (1994), 211-218.

[5] K. Boukir, Y. Maday, B. MéTivet, E. Razafindrakoto, A higer-order characteristics/finite element method for the incompressible Navier-Stokes equations, *Int. J. Numer. Math. Fluids*, **25** (1997), 1421-1454.

[6] K. Boukir, B. Nitrosso and B. Maury, A characteristics-ALE method for variable domain Navier-Stokes equations. In: L.C. Wrobel, B. Sarler, and C.A. Brebbia (eds.), *Computational Modelling*

of Free and Moving Boundary Problems III, Southampton/Boston: Comput. Mech. Publ., (1995), 57-65.

[7] C. Bruneau, M. Saad, The 2D lid-driven cavity problem revisited, *Computers & Fluids*, **35** (2006), 326-348.

[8] G.C. Buscaglia, E.A. Dari, Implementation of the Lagrange-Galerkin method for the incompressible for the incompressible Navier-Stokes equations, *Int. J. Numer. Methods Fluids*, **15** (1992), 23-36.

[9] Z.X. Chen, Characteristic mixed discontinuous finite element methods for advection-dominated diifusion problems, *Comput. Methods Appl. Mech. Engrg.*, **191** (2002), 2509-2538.

[10] Z.X. Chen, R.E. Ewing, Q. Jiang, A.M. Spagnuolo, Error analysis for characteristics-based methods for degenerate Parabolic problems, *SIAM J. Numer. Anal.*, **40** (4) (2002), 1491-1515.

[11] P.G. Ciarlet, *The Finite Element Method for Elliptic Problems*, NorthHolland, Amsterdam (1978).

[12] S. Collis, Montioring unresolved scales in multiscale turb lence modeling, *Phys. Fluids*, **13** (2001), 1800-1806.

[13] A. Corsini, F. Rispoli, A. Santoriello, A variational multiscale higher-order finite element formulation for turbomachinery flow computations, *Comput. Methods Appl. Mech. Engrg.*, **194** (2005), 4797-4823.

[14] C.N. Dawson, T.F. Russell, M.F. Wheeler, Some improved error estimates for the modified method of characteristics, *SIAM J. Numer. Anal.*, **26** (6) (1989), 1487-1512.

[15] J. Douglas Jr., F. Pereira, L.M. Yeh, A locally conservative Eulerian-Lagrangian numerical method and its application to nonlinear transport in porous media, *Comput. Geosci.*, **4** (2000), 1-40.

[16] J. Douglas Jr., T.F. Russell, Numerical methods for convection-dominaed diffusion problems based on combing the method of charateristics with finite element or finite difference procedures, *SIAM J. Numer. Anal.*, **19** (1982), 871-885.

[17] E. Erturk, T.C. Corke, C. Gökvöl, Numerical solutions of 2-D steady incompressible driven cavity flow at high Reynolds numbers, *Int. J. Numer. Meth. Fluids*, **48** (2005), 747-774.

[18] R.E. Ewing and T.F. Russell, Multistep Galerkin method along characteristics for convection-diffusion problems, in R. Vichnevestsky and R.S. Steoleman(eds), *Adv. Comput. Methods P.D.E.*, 1981, 28-36.

[19] Gravemeier V. The variational multiscale method for laminar and turbulent flow, *Arch. Comput. Met h. Engng.*, **13** (2006), 249-324.

[20] U. Ghia, K.N. Ghia, C.T. Shin, High-Re solution for incompressible flow using the Navier-Stokes equations and a multigrid method, *J. Comput. Physics*, **48** (1982), 387-411.

[21] V. Girault, P.A.Raviart, *Finite element method for Navier-Stokes equations: theory and algorithms*, Springer-Verlag, Berlin, Herdelberg, 1987.

[22] P. Hansbo, The characteristic streamline diffusion method for the time-dependent incompressible Navier-Stokes equations, *Comput. Methods Appl. Mech. Engrg.*, **99** (1992), 171-186.

[23] Y.N. He, W.W. Sun, Stability and convergence of the Crank-Nicolson/Adams-Bashforth scheme for the time-dependent Navier-Stokes equations, *SIAM J. Numer. Anal.*, **45** (2) (2007), 837-869.

[24] Y.N. He, J. Li, Convergence of three iterative methods based on the finite element discretization for the stationary Navier-Stokes equations, *Comput. Methods Appl. Mech. Engrg.*, **198** (2009), 1351-1359.

[25] Y.N. He, A.W. Wang, A simplified two-level method for the steady Navier-Stokes equations, *Comput. Methods Appl. Mech. Engrg.*, **197** (2008), 1568-1576.

[26] T. Hughes, Multiscale phenomena: Greens functions, the Dirichlet-to-Neumann formulation, subgrid scale models, bubbles and the origins of stabilized methods, *Comput. Methods Appl. Mech. Engrg.*, **127** (1995), 387-401.

[27] T.J.R. Hughes, G.R. Feijóo, L. Mazzei, J.B. Quincy, The variational multiscale method–a paradigm for computational mechanics, *Comput. Methods Appl. Mech. Engrg.*, **166** (1998), 3-24.

[28] T. Hughes, L. Mazzei, A. Oberai, A. Wray, The multiscale formulation of large eddy simulation: decay of homogeneous isotropic turbulence, *Phys. Fluids*, **13** (2001), 505-512.

[29] T. Hughes, A. Oberai, L. Mazzei, Large eddy simulation of turbulent channel flows by the variational multiscale method, *Phys. Fluids*, **13** (2001), 1784-1799.

[30] V. John, On large eddy simulation and variational multiscale me thods in the numerical simulation of turbulent incompressible flows, *Appl. Math.*, **4** (2006), 321-353.

[31] V. John, S. Kaya, A finite element variational multiscale method for the Navier-Stokes equations, *SIAM J. Sci. Comp.*, **26** (2005), 1485-1503.

[32] V. John, S. Kaya and W. Layton, A two-level variational multiscale method for convection-dominated convection-diffusion equations, *Comp. Meth. Appl. Math. Eng.*, **195** (2006), 4594-4603.

[33] V. John, S. Kaya, Finite element error analysis for a variational multiscale method for the Navier-Stokes equations, *Adv. Comput. Math.*, **28** (2008), 43-61.

[34] V. John, A. Kindl, Numerical studies of finite element variational methods for turbulent flow simulations, *Comput. Meth. Appl. Mech. Eng.*, **199** (2010), 841-852.

[35] V. John, A Kindl, A variational multiscale method for turbulent flow simulation with adaptive large scale space, *J. Comput. Phy.*, **229** (2010), 301-312.

[36] V. John, S. Kaya, A. Kindl, Finite element error analysis for a projection-based variational multiscale method wiyh nonlinear eddy viscosity, *J. Math. Anal. Appl.*, **344** (2008), 627-641.

[37] B. Koobus, C. Farhat, A variational multiscale method for the large eddy simulation of compressible turbulent flows on unstructured meshes–application to vortex shedding, *Comput. Methods Appl. Mech. Engrg.*, **193** (2004), 1367-1383.

[38] J. Li, Z.X. Chen, A new local stabilized non conforming finite element method for the Stokes equations, *Computing*, **82** (2008), 157-170.

[39] O. Pironnequ, On the transport-diffusion algorithm and it's applications to the Navier-Stokes equations, *Numer. Math.*, **38** (1982), 309-332.

[40] A. Quarteroni, A. Valli, *Numerical Approximation of Partial Differential Equations*, Springer-Verlag, World Publishing Co., 1998.

[41] T.F. Russell, Time stepping along charactercteristics with incomplete iteration for a Galerkin approximation of miscible displacement in prous media, *SIAM J. Numer. Anal.*, **22** (5) (1985), 970-1013.

[42] J. Sesterhenn, A characteristic-type formulation of the Navier-Stokes equations for high order upwind schemes, *Computers & Fluids*, **30** (2001), 37-67.

[43] Z.Y. Si, Second order modified method of characteristics mixed defect-correction finite element method for time dependent Navier-Stokes problems, Numer. Algor., 59(2) (2012), 271-300.

[44] E. Süli, Convergence and nonlinear stability of the Lagrange-Galerkin method for the Navier-Stokes equations, *Numer. Math.*, **53** (1998), 459-483.

[45] M. Venturin, R. Bertelle, M.R. Russo, An accelerated algorithm for Navier-Stokes equations,*Simulat. Modell. Pract. Theory*, **18** (2010), 217-229.

[46] Y. Zhang, Y.N. He, Assessment of subgrid-scale models for the incompressible Navier-Stokes equations, *J. Comput. Appl. Math.*, **234** (2010), 593-604.